

Novel Polymeric Scaffolds Using Protein Microbubbles as Porogen and Growth Factor Carriers

Ashwin Nair, M.S., Paul Thevenot, M.S., Jagannath Dey, M.S., Jinhui Shen, M.D.,
Man-Wu Sun, B.S., Jian Yang, Ph.D., and Liping Tang, Ph.D.

Polymeric tissue engineering scaffolds prepared by conventional techniques like salt leaching and phase separation are greatly limited by their poor biomolecule-delivery abilities. Conventional methods of incorporation of various growth factors, proteins, and/or peptides on or in scaffold materials via different crosslinking and conjugation techniques are often tedious and may affect scaffold's physical, chemical, and mechanical properties. To overcome such deficiencies, a novel two-step porous scaffold fabrication procedure has been created in which bovine serum albumin microbubbles (henceforth MB) were used as porogen and growth factor carriers. Polymer solution mixed with MB was phase separated and then lyophilized to create porous scaffold. MB scaffold triggered substantially lesser inflammatory responses than salt-leached and conventional phase-separated scaffolds *in vivo*. Most importantly, the same technique was used to produce insulin-like growth factor-1 (IGF-1)-eluting porous scaffolds, simply by incorporating IGF-1-loaded MB (MB-IGF-1) with polymer solution before phase separation. *In vitro* such MB-IGF-1 scaffolds were able to promote cell growth to a much greater extent than scaffold soaked in IGF-1, confirming the bioactivity of the released IGF-1. Further, such MB-IGF-1 scaffolds elicited IGF-1-specific collagen production in the surrounding tissue *in vivo*. This novel growth factor-eluting scaffold fabrication procedure can be used to deliver a range of single or combination of bioactive biomolecules to substantially promote cell growth and function in degradable scaffold.

Introduction

TISSUE ENGINEERING SCAFFOLDS play a critical role in tissue engineering by acting as a temporary tissue construct or building block for cell accommodation, proliferation, and differentiated function as well as serving as three-dimensional templates for neotissue/organ formation.¹ To create such a temporary structure for cell growth, degradable polymeric materials, such as poly (L-lactic acid) and poly (L-lactic-co-glycolic acid) (PLGA), are commonly used and have been extensively researched.^{2,3} In addition, many procedures have been developed for the preparation of porous matrices such as solvent casting/particulate leaching, emulsion freeze drying, gas foaming, and thermally induced phase separation.⁴⁻¹⁶ These methods allow us to produce a series of scaffolds with desired porosity and different physical/mechanical properties. However, most scaffolds fail to attract and grow a large number of cells mostly due to the lack of a suitable growth environment. To improve cell seeding and growth, substantial progress has been made in recent years by either coating the scaffold with different adhesive proteins like laminin, fibronectin, fibrin, collagen, and vitronectin,¹⁷⁻²⁰ or soaking the scaffold with various growth factors like insulin-like growth factor (IGF), transforming growth factor-β, platelet-derived

growth factor, and fibroblast growth factor via spontaneous adsorption or covalent linking.²⁰⁻²² These additional treatments improved cell growth, although such enhancements were often limited and short lived. It is also possible that common growth factor-scaffold conjugation processes may alter the morphological and physical strength of the scaffold. Thus, there is an urgent need to develop a new scaffold fabrication technique in which a variety of growth factors can be embedded and released for a prolonged period of time.

Quite a few studies have reported that growth factor-loaded nanoparticles are able to release a variety of growth factors for a long period of time.^{23,24} Despite impressive research progress, such growth factor-eluting particles may not be adopted as part of the porous scaffold fabrication processes. The main hurdle is that growth factors can be easily denatured or inactivated by organic solvents used for scaffold fabrication.^{25,26} Studies have also shown that scaffolds soaked in growth factors have a characteristic high burst release in the first 1–2 days. This occurs since most of the growth factor is bound to the surface, instead of being embedded inside the scaffold.²⁷ To reduce the direct contact between growth factor and solvent used in scaffold fabrication, our recent studies uncovered that albumin microbubbles (MB) can shield the encapsulated growth factors from solvent denaturation.

It should be noted that protein MB, especially albumin MB, have been widely used in the field of ultrasound imaging as a contrast agent,^{28–31} and gene delivery vehicles.^{32–35}

In this work, we tested the hypothesis that growth factor-releasing scaffolds can be fabricated by incorporating growth factor-releasing bovine serum albumin (BSA) MB in the scaffold-manufacturing processes. To test this hypothesis, we first determined whether albumin MB can be used as a new porogen to produce albumin-coated cell-friendly surfaces. For that, a series of studies were carried out to determine the ratios of albumin MB and PLGA polymer, quenching temperatures, and processing conditions to finally arrive at the best combination to synthesize scaffolds with optimal pore sizes. MB scaffolds were evaluated on the basis of their surface morphology, internal structure, and mechanical strength. The *in vitro* cell proliferation studies were conducted, and the *in vivo* performance of such scaffolds was compared with salt-leached and conventional phase-separated scaffolds. Second, a series of studies were carried out to evaluate the ability of MB porogens in preserving the bioactivity of a loaded growth factor. IGF-1 was chosen as model growth factor, since it stimulates fibroblastic 3T3 cell proliferation.^{36–38} The bioactivity of the IGF-1 released from the scaffolds was determined in both an *in vitro* cell culture system and *in vivo* animal implantation model.

Materials and Methods

Materials

Poly (D,L-lactic-co-glycolic acid) (75:25) with a molecular weight of 113 kDa was purchased from Medisorb (Lakeshore Biomaterials, Birmingham, AL). The solvent 1,4-dioxane and Coomassie blue was obtained from Aldrich (Milwaukee, WI) and EMD Biosciences (Darmstadt, Germany), respectively. Masson's trichrome kit and BSA were bought from Sigma (St. Louis, MO).

Preparation of BSA MB and IGF-loaded MB

BSA MB were produced based on an established procedure.^{28–31} Briefly, 5% w/v solution of BSA was overlaid with nitrogen gas. The mixture was sonicated using a probe sonicator (Ultrasonix, Bothell, WA) at 20 kHz for 10 s. This procedure resulted in the formation of nitrogen gas-filled MB that were surrounded by a BSA protein shell. The MB were transferred to glass tubes and kept at 4°C. To observe the physical structure of MB, a small droplet of the MB was placed on a glass slide and then imaged under a microscope (Leica Microsystems, Wetzlar, Germany). The MB size distribution was determined using the images and NIH Image^j.³⁹ To synthesize IGF-1-loaded MB (labeled as MB-IGF-1), IGF-1 (500 ng/mL) solution was mixed with BSA solution before sonication under nitrogen gas as described earlier.

Fabrication of MB-embedded porous scaffolds

BSA MB-embedded porous scaffold (labeled as MB scaffold) was produced based on a modified phase separation procedure. In our pilot studies, different concentrations of BSA (5% w/v, 10% w/v, 20% w/v, and 50% w/v) were used to synthesize the MB and different loading amounts (1:1 and 1:2) of MB were added into various concentrations of polymer solution (5% w/v, 7.5% w/v, and 10% w/v). Such MB-

polymer mixtures were phase separated at various temperatures (0°C, -20°C, and -196°C). The technique was optimized based on the information obtained from these studies and in this work. Briefly, 7.5% w/v PLGA was dissolved in 1,4-dioxane by vortexing for about 20 min till the polymer completely dissolved in the solvent. The polymer solution was then mixed with the BSA MB (5% w/v BSA) or water (as negative control) in a ratio of 1:1. After gentle agitation for 3 min at room temperature, the polymer-solution mixtures in glass Petri dishes (5 cm diameter) were then quenched in liquid nitrogen to induce phase separation. The solidified scaffolds were then lyophilized for 48 h at 0.03 mbar vacuum in a Freezone 12 lyophilizer (Labconco, Kansas City, MO). As comparison, conventional phase-separated scaffolds and salt-leached scaffolds were also synthesized as described earlier.^{2,40}

For producing IGF-1-loaded, MB-embedded scaffolds, IGF-1-loaded MB (MB-IGF-1, MB manufactured in the presence of 500 ng/mL IGF-1) were used as porogens. To directly test the influence of MB on IGF-1 release, some phase-separated scaffolds were soaked in 500 ng/mL IGF-1 at 4°C overnight, and these IGF-1-soaked scaffolds were used in some studies as controls.

Scaffolds characterization

To determine the potential contribution of BSA MB in creating porosity in scaffold, a staining method was developed to view the location of BSA bubbles after scaffold fabrication procedure. For that, variously manufactured scaffolds were immersed with freezing medium Tissue-Tek OCT (Sakura FineTek, Torrance, CA) and then placed under vacuum at -70 kPa, for 15 min to facilitate the perfusion of the freezing medium through the pores of the scaffold. After freezing overnight, the scaffolds were sectioned in a cryostat (Leica CM1850; Leica Microsystems) and collected on poly (L-lysine)-treated slides. To view MB distribution, 10 µm scaffold sections were obtained and then stained with Coomassie brilliant blue solution (0.1% w/v of Coomassie blue dye, 45% w/v methanol, 45% w/v water, and 10% w/v acetic acid) for 4 min. Destaining to remove unbound dye was accomplished by dipping the sections in destaining solution (10% w/v methanol, 10% w/v acetic acid, and 80% w/v water).² The slides were observed under a Leica microscope (Leica Microsystems) equipped with a CCD camera (Retiga EXi; Qimaging, Surrey BC, Canada). Surface morphology of the cross sections of the scaffolds (60 µm thickness) was also observed using a Hitachi 3000N scanning electron microscope (Hitachi High Tech, Tokyo, Japan).

The porosity of the scaffolds was determined by ethanol displacement method based on a published procedure.⁴¹ Mechanical testing was conducted with an MTS Insight 2 machine fitted with a 500 N load cell. The samples were cut into square discs (6.3 mm width × 6.5 mm thickness). The deflection rate was adjusted to 2 mm/min. Samples were compressed to 10% strain. The Young's modulus was calculated from the initial slope of the curve.⁴²

Evaluation of scaffolds suitability for *in vitro* cell culture

For *in vitro* cell growth study, square sections (1×1×1 cm) of both phase-separated scaffold and the protein MB scaffolds were soaked in ethanol for few minutes followed by

multiple washes with sterile PBS. Scaffolds were seeded with 3T3 cells (5×10^5 /sample in Dulbecco's modified Eagle's medium (DMEM) with 10% fetal calf serum and 1% antibiotics) using a dynamic cell seeding technique ($n=4$).⁴⁰ The cell-seeded discs were then supplemented with DMEM and placed in a new culture well in an incubator under 37°C and 5% CO₂. After culturing for 7 days, the cell viability and proliferation on the scaffolds was determined using an MTS assay.⁴⁰

Measurements of IGF-1 bioactivity

The ability of BSA MB to protect the bioactivity of growth factor was determined using an IGF-1 bioactivity assay. First, an IGF bioactivity assay was established using a 3T3 cell proliferation assay. Specifically, different concentrations (50, 200, and 500 ng/mL) of IGF-1 were added to 3T3 cells plated at a density of 10,000 cells/well in 24-well tissue culture dishes and incubated for 4 days. After 4 days MTS cell proliferation assay was performed to determine the linear relationship between IGF-1 concentrations and cell numbers.

To determine the protective function of MB on IGF-1 activity, IGF-1-loaded MB, MB alone, and IGF alone (as negative) were exposed to 1,4-dioxane and lyophilized. The dry residuals were resuspended in 1 mL DMEM. The residual IGF-1 bioactivity was then determined as described above.

To assess the release of bioactive IGF-1 from scaffold, MB-IGF-1 scaffolds and IGF-1-soaked phase-separated scaffolds were incubated at 37°C with 1 mL DMEM that served as a release medium. At various time intervals (12 h and 1, 2, 3, 4, 5, and 6 days), the incubated medium was collected for bioactivity assay, and a fresh medium was then added. At the end of the study, the extent of IGF-1 bioactivity in the medium was determined using IGF-1 bioactivity assay.

In vivo evaluation of scaffolds

To evaluate the *in vivo* biocompatibility, square sections (1 cm length \times 1 cm breadth \times 1 cm thickness) of salt-leached, phase-separated control, and MB scaffolds were implanted in the dorsal subcutaneous region of BALB/c mice (25 g body weight) from Harlan (Indianapolis, IN). After implantation for 7 days, the animals were sacrificed and the tissue was explanted. The tissue responses to scaffold implants were then analyzed histologically. Animals were cared for in compliance with protocols approved by the Institutional Animal Care and Use Committee (IACUC) at the University of Texas at Arlington.

Histological analyses

All tissue samples were frozen and sectioned into 10-μm-thick sections using a Leica Cryostat (CM1850) (Leica Microsystems). To assess the extent of gross inflammatory responses to the implants, some of the tissue sections were stained with hematoxylin and eosin. Microscopic images of hematoxylin and eosin-stained slides were used to assess the extent of implant-mediated fibrotic responses by measuring the extent of fibrotic tissue thickness. To assess the bioactivity of the released IGF-1, some of the tissue sections were stained with Masson's Trichrome blue in which nuclei stains blue-black and collagen stains blue.⁴³ The relative intensity of trichrome blue was determined using the Measure RGB feature in NIH ImageJ and was expressed in arbitrary units per square mm.³⁹

Statistical analysis

Data are expressed as mean \pm standard deviation. The statistical significance between two sets of data was calculated using two-tailed Student's *t*-test. Data were considered significant when $p < 0.05$ or $p < 0.01$ was obtained.

Results

BSA MB characterization

BSA MB were synthesized and then used as growth factor carrier and tissue scaffold porogen. After sonication, 1 mL of BSA solution usually generated 0.8 mL of MB. The synthesized MB observed under the microscope revealed a core-shell structure (Fig. 1a) and had a size range of 100–150 μm (Fig. 1b). The protein shell coupled with the low diffusivity nitrogen gas ensured that the MB are stable at room temperature and can be stored at 4°C for up to 2 h. The supplement of IGF-1 in the process allowed the production of IGF-loaded MB. IGF-loaded MB exhibited similar morphology and size distribution as control BSA MB.

Synthesis and characterization of MB-embedded tissue scaffolds

By observing the cross sections of the MB-embedded PLGA scaffolds under the scanning electron microscope, we found that, without the addition of MB, phase-separated scaffold shows typical ladder-like porous structure with pore sizes ranging 10–30 μm (Fig. 2a, b). On the other hand, MB-embedded scaffolds have open porous structure similar to salt-leached scaffolds. In addition, the pore sizes of MB scaffold were much larger ranging from 100 to 150 μm (Fig. 2c, d).

Under the scanning electron microscope, consistent with surface morphology, control phase-separated scaffolds showed an internal microporous structure in the range of 10–20 μm (Fig. 3a), and BSA MB-embedded scaffold showed the presence of large pores, almost 10 times greater than conventional phase-separated scaffolds, measuring around 100–200 μm in diameter (Fig. 3b). To further determine the role of MB in scaffold porosity, the distribution of MB in scaffolds was viewed using Coomassie blue stain, which labels the protein with dark blue color. Indeed, almost all of the walls of large pores stained positive with Coomassie blue stain (Fig. 3d). As expected, such localized Coomassie blue stain could not be found in control scaffold as no protein was added during the fabrication (Fig. 3c). These results support our idea that BSA MB can be used as porogens to create homogenous large-sized pore distribution throughout tissue scaffold.

Porosity and mechanical strength of MB-embedded scaffolds

To allow cell growth and tissue transplantation, it is critical that the MB-embedded scaffold have high porosity and good mechanical strength. We found that the porosity of the MB-loaded scaffolds was comparable to that of the control phase-separated scaffolds (almost 92%) (Fig. 4a). These results suggest that the increase of pore size does not affect the overall porosity of the scaffold. However, large pore size may weaken the mechanical strength of the scaffold as seen in the compressive strength analysis of MB-embedded scaffolds compared to controls (Fig. 4b).

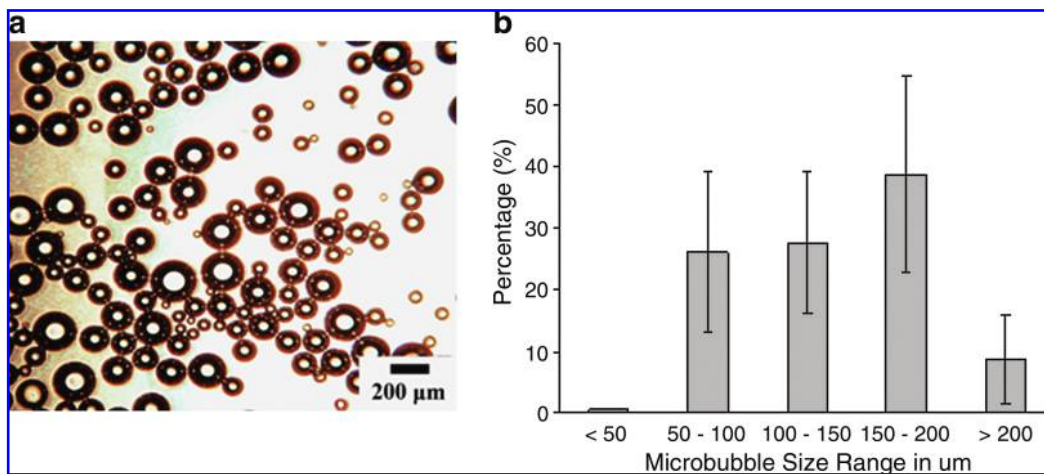


FIG. 1. Microbubbles (MB) were placed on glass slides and observed under a light microscope. Optical images of the protein MB (**a**) was used to determine the size range distribution of the MB (**b**) (magnification, 100 \times ; scale bar = 200 μm). Color images available online at www.liebertonline.com/ten.

In vitro cell toxicity of MB-embedded scaffolds

Although BSA MB have been shown to be very biocompatible and have low cell cytotoxicity, it is not clear whether scaffold fabrication procedure would affect the biocompati-

bility and cell compatibility of BSA MB. To find the answer, both phase-separated scaffolds and MB-embedded scaffolds were seeded with 5×10^5 3T3 cells/scaffold, and the proliferation of seeded cells on different scaffold was then determined. Surprisingly, we found that the incorporation of BSA

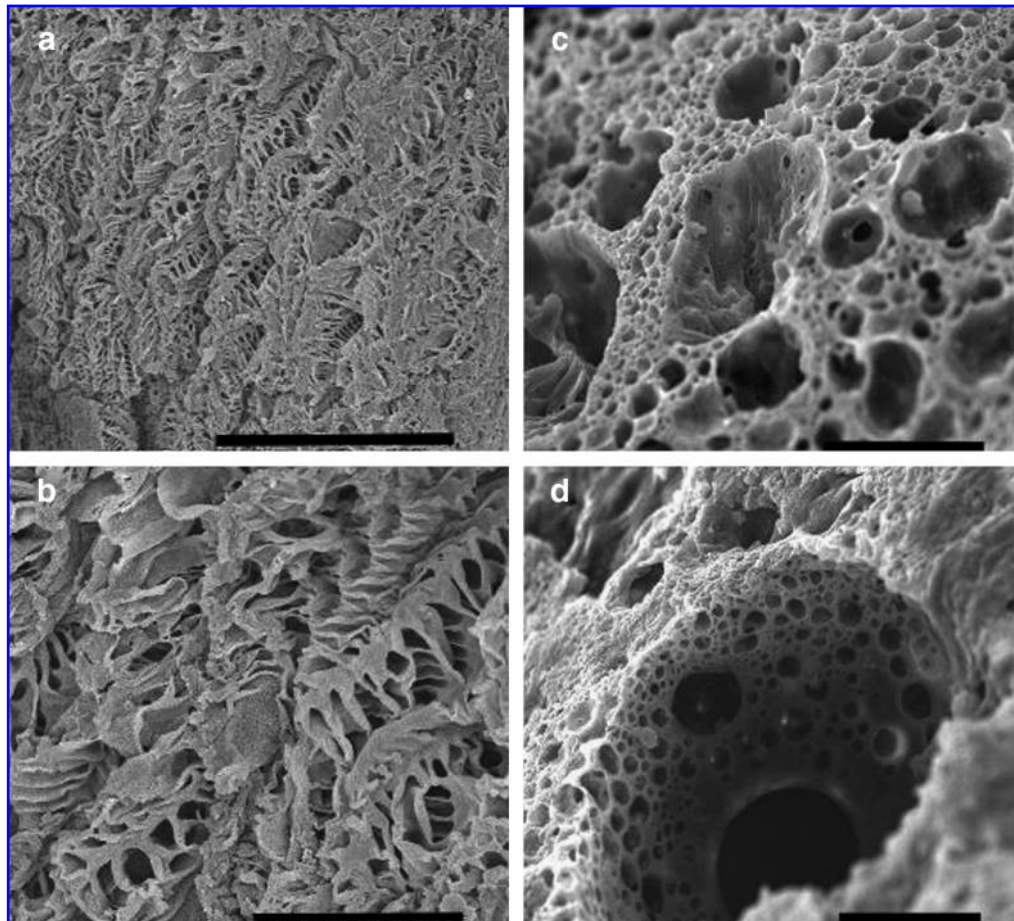


FIG. 2. Scanning electron microscopy analysis shows the porous structures of control phase-separated scaffold with small pores in lower (**a**) and higher magnifications (**b**). On the other hand, bovine serum albumin (BSA) MB scaffold showed large pores and honeycomb-like pore-wall structure in lower (**c**) and higher (**d**) magnifications (scale bars = 100 μm).

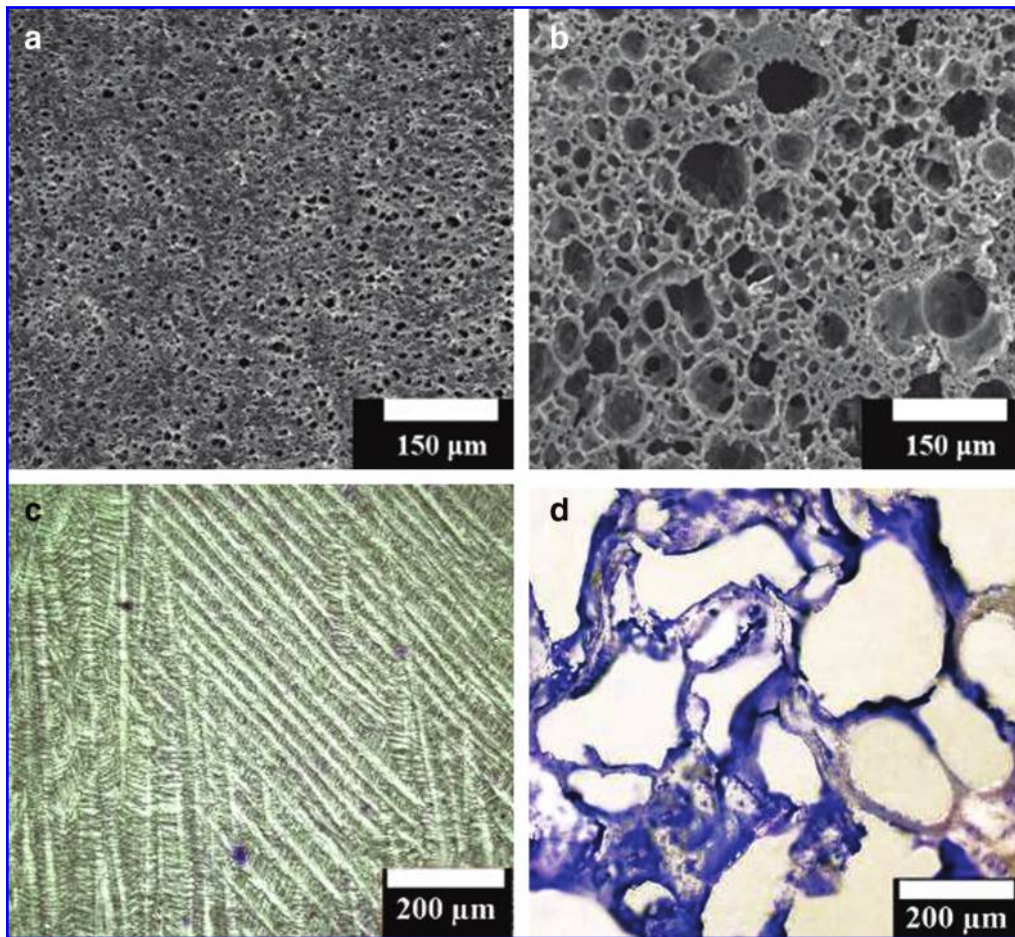


FIG. 3. The cross-sectional images of phase-separated scaffold in the presence or absence of BSA MB. The morphology of control phase-separated scaffolds (a) and BSA MB scaffolds (b) was observed under the scanning electron microscope. To view the distribution of the MB in scaffold, scaffold sections were stained with Coomassie blue and observed under an optical microscope. Control phase-separated scaffolds (c) and MB-embedded scaffolds (d) (magnification, 200 \times). Color images available online at www.liebertonline.com/ten.

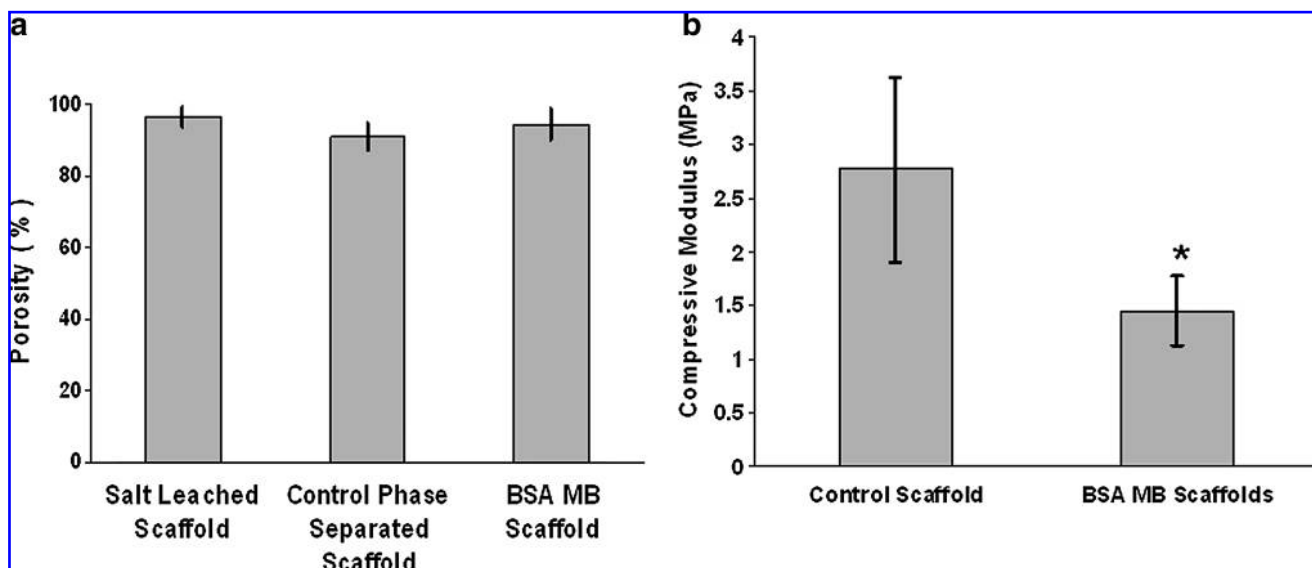


FIG. 4. Physical and mechanical characterization of MB-embedded scaffolds. The porosity of the scaffolds was determined by ethanol displacement method and compared with control phase-separated scaffolds (a). Mechanical strength of MB-embedded scaffolds was compared with control phase-separated scaffolds using an MTS mechanical tester (b). * $p < 0.05$.

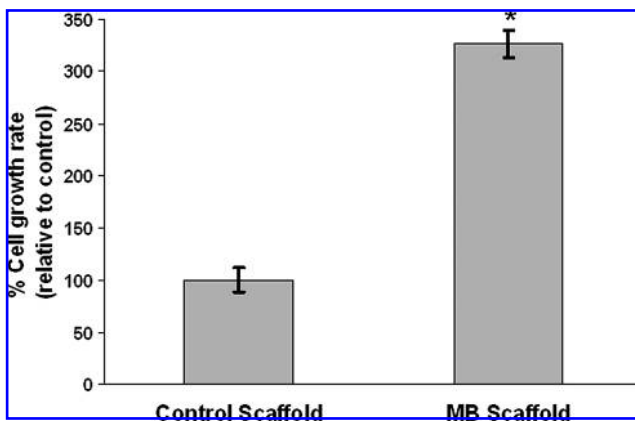


FIG. 5. Growth rate of 3T3 cells on phase-separated scaffold and MB-embedded scaffold (MB scaffold). Cells were grown on phase-separated scaffolds (control) and MB scaffolds for 7 days, and percentage cell growth rates were determined relative to control. $*p < 0.05$.

MB in fact enhanced the cell proliferation by almost three times as compared with the control scaffolds (Fig. 5).

In vivo tissue compatibility of MB-embedded scaffolds

Using mouse subcutaneous implantation model, we compared the tissue compatibility of MB-embedded scaffolds with two commonly used scaffolds—salt-leached scaffolds and phase-separated scaffolds made of the same materials. Salt-leached scaffolds (average pore size of 250 μm), phase-separated controls (pore size range, 10–20 μm), and MB-embedded scaffolds (pore size range, 100–120 μm) had comparable porosity (90–94%). In agreement with earlier

observations, prominent fibrotic tissue formation was found surrounding salt-leached (Fig. 6a) and phase-separated scaffolds (Fig. 6b). However, there was a significant reduction in the fibrotic tissue reaction elicited by the MB-embedded scaffolds (Fig. 6c). The statistical analyses confirmed our observations (Fig. 6d).

Retention of IGF-1 bioactivity by BSA MB

MB have been used to sheath growth factors and genetic materials from the inactivation of host enzymes and protein antagonists. We thus assumed that MB may be able to embed growth factors in scaffold and also protect their bioactivity from solvent denaturation during scaffold fabrication process. To test this hypothesis, IGF-1 was used as a model protein and a cell culture bioassay was established to determine the bioactivity of IGF-1. The results from our pilot studies have found that 500 ng/mL is the optimum concentration of IGF-1 for triggering maximum cell proliferation. We then determined whether MB can shield the growth factor from organic solvent inactivation. For that, solutions of IGF-1, BSA MB, and BSA MB loaded with IGF-1 (MB-IGF-1) (500 ng/mL) were added to organic solvent 1,4-dioxane, frozen, and lyophilized. Postlyophilization, DMEM was added to each group and then used in IGF-1 bioassays. As expected, IGF-1 alone lost almost all its bioactivity after being exposed to solvent. Solvent-incubated MB exerted minimal cell proliferation activity (Fig. 7a). Most importantly, IGF-1 sheltered in MB was found to retain most of its bioactivity (before vs. after solvent exposure: 500 ± 5 ng/mL vs. 150 ± 10 ng/mL). These results support our hypothesis that MB shield loaded growth factors from solvent inactivation.

We further determined whether growth factor-releasing scaffold can be made using MB-embedded scaffold fabrica-

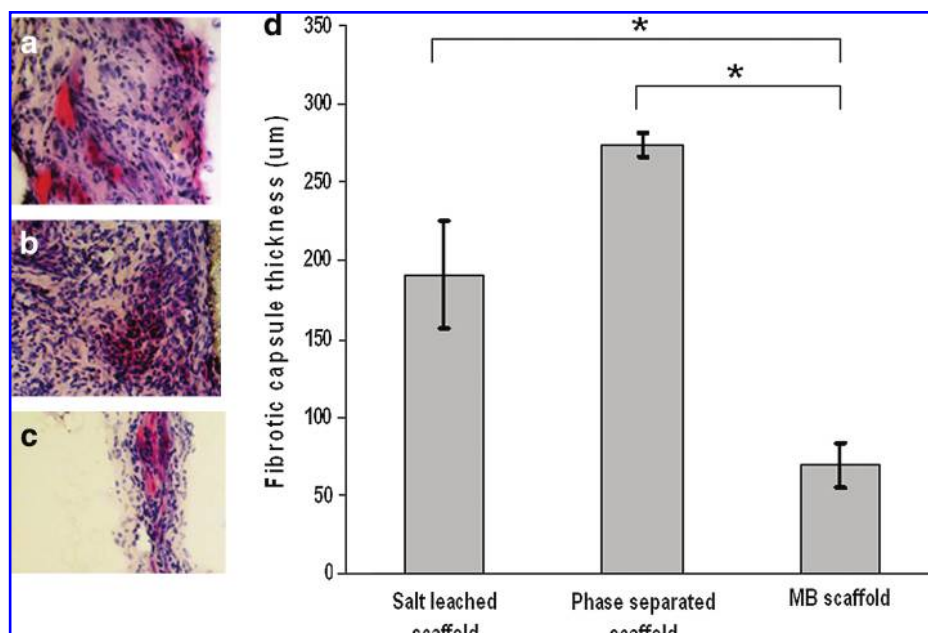


FIG. 6. *In vivo* histological analysis of fibrotic tissue reactions surrounding MB scaffolds (a) compared to salt-leached (b) and phase-separated scaffolds (c). All images were taken at 200 \times magnification with scaffold toward the right edge of the tissues. Fibrotic capsule thickness measured using NIH ImageJ was quantified to reflect the extent of implant-mediated tissue responses (d). $*p < 0.05$. Color images available online at www.liebertonline.com/ten.

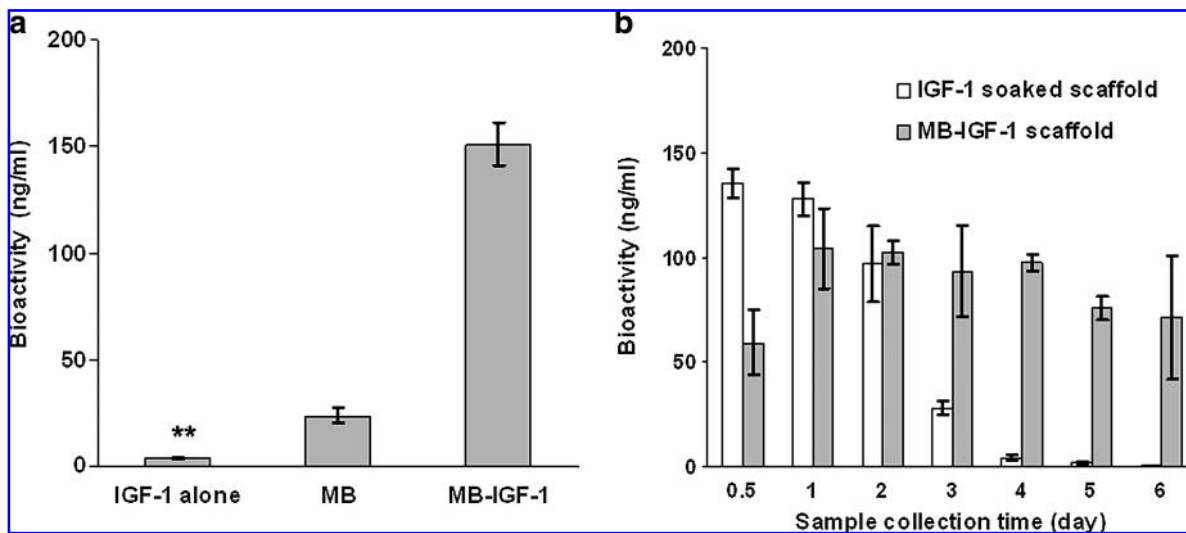


FIG. 7. Insulin-like growth factor-1 (IGF-1) bioactivities of variously treated samples were measured based on cell proliferation assay. The effect of solvent on IGF-1 bioactivity was determined using solvent-preexposed IGF-1 alone, MB alone, and MB-IGF-1 as explained in methods (significance vs. MB control; ** $p < 0.01$) (a). The bioactivity of released IGF-1 from MB-IGF-1 scaffolds and IGF-1-soaked scaffolds at different time points was assessed as shown in (b).

tion technique. IGF-1-coated phase-separated scaffolds were used as negative controls. Both groups of scaffolds were incubated with DMEM with daily changes of fresh medium. The bioactivity of IGF-1 in the collected medium was then determined based on cell proliferation assay (Fig. 7b). In the case of IGF-1-coated scaffold, most of IGF-1 release occurred before day 1 and then dropped sharply. By day 3, there was almost no bioactive IGF-1 release from scaffold. On the other hand, MB-IGF-1-embedded scaffold showed a prolonged release of IGF-1 for at least 6 days. These results demonstrate that MB can be used to fabricate growth factor-releasing scaffold.

In vivo bioactivity of IGF-1 and biocompatibility evaluation of scaffolds

Further studies were carried out to assess the effect of MB-IGF-1-embedded scaffold on tissue responses using a mouse subcutaneous implant model. Since IGF-1 has been shown to enhance fibroblast proliferation and collagen production, the *in vivo* bioactivity of IGF-1 was assessed by histologically analyzing the extent of collagen production surrounding scaffold implants. The capsule region around the salt-leached (Fig. 8a) and phase-separated scaffold (Fig. 8b) showed sparse collagen formation after implantation for 1 week, while low degree of collagen was found surrounding the MB scaffolds (Fig. 8c). However, as anticipated, the MB-IGF-1 scaffolds (Fig. 8d) showed a well-formed band of collagen around the implants. The quantitative analysis of the collagen deposition (based on intensity of collagen blue stain) confirmed the visual observations (Fig. 8e). These results clearly demonstrated the ability of MB-IGF-1 scaffold to release bioactive IGF-1 and to affect the surrounding tissue responses.

Discussion

Ensuring the bioactivity of growth factors and other biomolecules delivered by scaffolds is one of the major hurdles

in tissue engineering.^{44–47} This challenge arises primarily due to the incompatibility between proteins and organic solvents used in fabricating scaffolds. Using nitrogen gas-filled BSA MB as porogen, a novel scaffold fabrication technique has been established here to produce porous and growth factor-releasing scaffold.

For fabricating MB-embedded scaffold, phase separation technique was used since the technique yields scaffolds with high porosity and interconnectivity albeit with small pores.² MB were found to be stable at low temperature and could be lyophilized and then resuspended.²⁸ Our studies have shown that MB are easy to synthesize and incorporate in scaffold. It should be noted that MB are stable at room temperature possibly due to the superior stability of protein coating around the bubble as suggested by earlier studies.²⁸ In addition, earlier studies have shown that nitrogen gas with low diffusivity has been used commercially (such as Imagent, AF0150) to stabilize the MB.⁴⁸ The stability of MB may be further improved using lower diffusivity gases like sulfur hexafluoride and perfluorocarbons.⁴⁹

The porosity of MB-embedded scaffold was found to be easily engineered by altering the polymer concentration and volume ratio between polymer solution and MB. Interestingly, the overall porosity of MB-embedded scaffold is very comparable to phase-separated and salt-leached scaffolds, which are in agreement with earlier studies.^{2,10,16} Despite similar porosity, the cross sections of MB scaffolds showed a honeycomb-like open pore wall structure with large pores (100–150 μm) differing from smaller, ladder-like pores (10–20 μm) found in the control phase-separated scaffold as shown in many previous work.^{16,50,51} The small, ladder-like pores are formed by dioxane crystals formed during the quenching process.¹⁶ The larger, honeycomb-like opened pores can possibly be attributed to the protein MB based on several lines of evidence. First, the large pore size and MB have a similar size range (100–150 μm). Second, large pores coincide with Coomassie blue protein staining,^{2,52} indicating

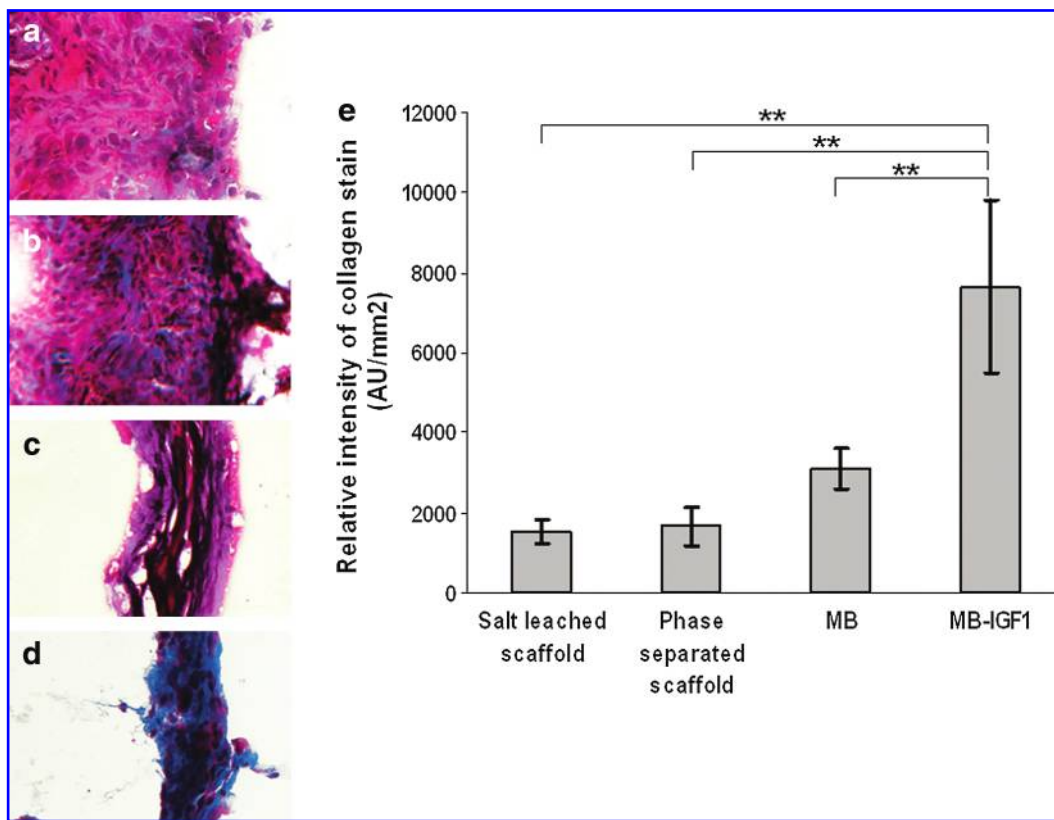


FIG. 8. *In vivo* bioactivity of IGF-1 was determined based on collagen production. Tissue sections were histologically analyzed using Masson's trichrome blue staining (collagen stain), where the blue coloration indicates presence of collagen (scaffold is to the right of fibrotic tissue). The fibrotic capsules around salt-leached (a), phase-separated (b), and MB scaffolds (c) were compared with MB-IGF1 scaffolds (d). All images were taken at a magnification of 200×. The quantitative analysis of collagen deposition was done based on intensity of blue color using NIH ImageJ (e). ** $p < 0.01$. Color images available online at www.liebertonline.com/ten.

that large pores are co-located with MB. Third, BSA MB-embedded scaffolds possess high cell seeding affinity, which is a typical property found on BSA-coated scaffolds.⁵³ This structural difference between phase-separated, salt-leached, and MB-embedded scaffolds may contribute to the visual perception of the vast dissimilarity in scaffold porosity. We have also noticed that the mechanical strength of the MB scaffolds is slightly weaker than control scaffolds. Although the main cause of such mechanical property change has yet to be determined, the large pores created by MB are likely to be the reason.

Using an *in vivo* implantation model, MB scaffolds were found to be more tissue compatible than salt-leached and phase-separated scaffolds with similar porosities. The improved tissue compatibility is likely to be associated to the presence of MB for the following reasons. First, BSA has been shown to block or limit unfavorable protein adsorption/denaturation, which is thought to be a major initiating step in the inflammatory response.⁵⁴ Second, albumin coating has been shown to reduce inflammatory responses to tissue scaffolds and polymeric materials.^{54–56}

Further studies have revealed that MB cannot only be used as porogen but also as a growth factor carrier. Although MB have been shown to protect proteins and activity of genetic material,³³ the ability of MB to protect the bioactivity of

growth factors during scaffold fabrication procedure had not been determined. In fact, our *in vitro* studies have shown that the bioactivity of IGF-1 was preserved when embedded in MB. Further, growth factor-releasing scaffold can be made following similar scaffold fabrication process with growth factor-loaded MB. This two-step process enables fabrication of a variety of growth factor-eluting scaffolds that is substantially simple and versatile compared to commonly used loading methods.^{20–22}

This MB scaffold fabrication technique provides a unique opportunity to explore the effect of a wide variety of growth factors in different tissue engineering application, tissue regeneration, and wound healing processes. Specifically, the slow release of VEGF⁵⁷ and b-FGF⁵⁸ has been shown to enhance angiogenesis. Such growth factor-loaded scaffolds can also be used for bone tissue engineering (requires pore sizes of 100–150 µm).⁵⁹ Similar techniques can be used to make scaffolds that could deliver neurotrophic factors and guide nerve regeneration.⁶⁰ Since it has been shown that protein MB could preserve the activity of loaded genetic material,³³ it is possible that scaffolds loaded with such MB can bring about the desired genetic modification in the seeded cells. We believe that further studies and developments of this novel fabrication technique may lead to the development of more cell and histocompatible tissue engineering products.

Conclusion

A novel and simple technique has been developed to load a variety of growth factors into tissue engineering scaffolds and deliver them in a bioactive form over time. This technique provides two distinct advantages. First, albumin MB are made of biological materials that have no toxicity and provide biocompatible coating along the pores throughout the scaffolds. Second, apart from having produced scaffolds with larger pores compared to conventional methods, our method permits the production of a wide variety of growth factor without the requirement of tedious fabrication processes. Such scaffold fabrication techniques could provide powerful tool for a whole range of tissue engineering applications.

Acknowledgment

This work was supported by NIH Grants RO1 GM074021 and EB007271.

Disclosure Statement

No competing financial interests exist.

References

1. Sahoo, S., Ouyang, H., Goh, J.C., Tay, T.E., and Toh, S.L. Characterization of a novel polymeric scaffold for potential application in tendon/ligament tissue engineering. *Tissue Eng* **12**, 91, 2006.
2. Nam, Y.S., and Park, T.G. Porous biodegradable polymeric scaffolds prepared by thermally induced phase separation. *J Biomed Mater Res* **47**, 8, 1999.
3. Ho, M.H., Kuo, P.Y., Hsieh, H.J., Hsien, T.Y., Hou, L.T., Lai, J.Y., and Wang, D.M. Preparation of porous scaffolds by using freeze-extraction and freeze-gelation methods. *Biomaterials* **25**, 129, 2004.
4. Yang, S., Leong, K.F., Du, Z., and Chua, C.K. The design of scaffolds for use in tissue engineering. Part I. Traditional factors. *Tissue Eng* **7**, 679, 2001.
5. Mikos, A.G., and Temenoff, J.S. Formation of highly porous biodegradable scaffolds for tissue engineering. *Electron J Biotechnol* **3**, 114, 2000.
6. Mikos, A.G., Thorsen, A.J., Czerwonka, L.A., Bao, D., Langer, R., Winslow, D.N., and Vacanti, J.P. Preparation and characterization of poly(L-lactic acid) foams. *Polymer* **35**, 1068, 1994.
7. Shastri, V.P., Martin, I., and Langer, R. Macroporous polymer foams by hydrocarbon templating. *Proc Natl Acad Sci USA* **97**, 1970, 2000.
8. Mooney, D.J., Mazzoni, C.L., Breuer, C., McNamara, K., Hern, D., and Vacanti, J.P. Stabilized polyglycolic acid fibre-based tubes for tissue engineering. *Biomaterials* **17**, 115, 1996.
9. Nam, Y.S., Yoon, J.J., and Park, T.G. A novel fabrication method of macroporous biodegradable polymer scaffolds using gas foaming salt as a porogen additive. *J Biomed Mater Res Appl Biomater* **53**, 1, 2000.
10. Hua, F.J., Kim, G.E., Lee, J.D., Son, Y.K., and Lee, D.S. Macroporous poly(L-lactide) scaffold 1. Preparation of a macroporous scaffold by liquid—liquid phase separation of a PLLA—dioxane—water system. *J Biomed Mater Res* **63**, 161, 2002.
11. Ma, P. Scaffolds for tissue fabrication. *Mater Today* **7**, 30, 2004.
12. Freed, L.E., Marquis, J.C., Nohria, A., Emmanuel, J., Mikos, A.G., and Langer, R. Neocartilage formation *in vitro* and *in vivo* using cells cultured on synthetic biodegradable polymers. *J Biomed Mater Res Appl Biomater* **27**, 11, 1993.
13. Mikos, A.G., Bao, Y., Cima, L.G., Ingber, D.E., Vacanti, J.P., and Langer, R. Preparation of poly (glycolic acid) bonded fiber structures for cell attachment and transplantation. *J Biomed Mater Res Appl Biomater* **27**, 183, 1993.
14. Mooney, D.J., Baldwin, D.F., Suh, N. P., Vacanti, J.P., and Langer, R. Novel approach to fabricate porous sponges of poly(D,L-lactic-co-glycolic acid) without the use of organic solvents. *Biomaterials* **17**, 1417, 1996.
15. Nam, Y.S., and Park, T.G. Biodegradable polymeric microcellular foams by modified thermally induced phase separation method. *Biomaterials* **20**, 1783, 1999.
16. Tu, C., Cai Q., Yang, J., Wan, Y., Bei, J., and Wang, S. The fabrication and characterization of poly(lactic acid) scaffolds for tissue engineering by improved solid–liquid phase separation. *Polym Adv Technol* **14**, 565, 2003.
17. Thomas, C.H., McFarland, C.D., Jenkins, M.L., Rezania, A., Steele, J.G., and Healy, K.E. The role of vitronectin in the attachment and spatial distribution of bone-derived cells on materials with patterned surface chemistry. *J Biomed Mater Res* **37**, 81, 1997.
18. Bhati, R.S., Mukherjee, D.P., McCarthy, K.J., Rogers, S.H., Smith, D.F., and Shalaby, S.W. The growth of chondrocytes into a fibronectin-coated biodegradable scaffold. *J Biomed Mater Res* **56**, 74, 2001.
19. Sales, V.L., Engelmayr, G.C., Jr., Johnson, J.A., Jr., Gao, J., Wang, Y., Sacks, M.S., and Mayer, J.E., Jr. Protein pre-coating of elastomeric tissue-engineering scaffolds increased cellularity, enhanced extracellular matrix protein production, and differentially regulated the phenotypes of circulating endothelial progenitor cells. *Circulation* **116**, 155, 2007.
20. Tessmar, J.K., and Gopferich, A.M. Matrices and scaffolds for protein delivery in tissue engineering. *Adv Drug Deliv Rev* **59**, 274, 2007.
21. Mann, B.K., Schmedlen, R.H., and West, J.L. Tethered-TGF-beta increases extracellular matrix production of vascular smooth muscle cells. *Biomaterials* **22**, 439, 2001.
22. Blunk, T., Sieminski, A.L., Gooch, K.J., Courter, D.L., Hollander, A.P., Nahir, A.M., Langer, R., Vunjak-Novakovic, G., and Freed, L.E. Differential effects of growth factors on tissue-engineered cartilage. *Tissue Eng* **8**, 73, 2002.
23. Hu, Y., Hollinger, J.O., and Marra, K.G. Controlled release from coated polymer microparticles embedded in tissue-engineered scaffolds. *J Drug Target* **9**, 431, 2001.
24. Eley, J.G., and Mathew, P. Preparation and release characteristics of insulin and insulin-like growth factor-one from polymer nanoparticles. *J Microencapsul* **24**, 225, 2007.
25. Fransson, J., Hallen, D., and Florin-Robertsson, E. Solvent effects on the solubility and physical stability of human insulin-like growth factor I. *Pharm Res* **14**, 606, 1997.
26. van de Weert, M., Hennink, W.E., and Jiskoot, W. Protein instability in poly(lactic-co-glycolic acid) microparticles. *Pharm Res* **17**, 1159, 2000.
27. Murphy, W.L., Peters, M.C., Kohn, D.H., and Mooney, D.J. Sustained release of vascular endothelial growth factor from mineralized poly(lactide-co-glycolide) scaffolds for tissue engineering. *Biomaterials* **21**, 2521, 2000.
28. Klibanov, A.L. Targeted delivery of gas-filled microspheres, contrast agents for ultrasound imaging. *Adv Drug Deliv Rev* **37**, 139, 1999.
29. Cosgrove, D. Why do we need contrast agents for ultrasound? *Clin Radiol* **51 Suppl 1**, 1, 1996.

30. Mulvagh, S.L., DeMaria, A.N., Feinstein, S.B., Burns, P.N., Kaul, S., Miller, J.G., Monaghan, M., Porter, T.R., Shaw, L.J., and Villanueva, F.S. Contrast echocardiography: current and future applications. *J Am Soc Echocardiogr* **13**, 331, 2000.
31. Czitrom, D., Karila-Cohen, D., Brochet, E., Juliard, J.M., Faraggi, M., Aumont, M.C., Assayag, P., and Steg, P.G. Acute assessment of microvascular perfusion patterns by myocardial contrast echocardiography during myocardial infarction: relation to timing and extent of functional recovery. *Heart* **81**, 12, 1999.
32. Russell, S.J. Science, medicine, and the future. *Gene therapy*. *BMJ* **315**, 1289, 1997.
33. Frenkel, P.A., Chen, S., Thai, T., Shohet, R.V., and Grayburn, P.A. DNA-loaded albumin microbubbles enhance ultrasound-mediated transfection *in vitro*. *Ultrasound Med Biol* **28**, 817, 2002.
34. Newman, C.M., and Bettinger, T. Gene therapy progress and prospects: ultrasound for gene transfer. *Gene Ther* **14**, 465, 2007.
35. Ferrara, K., Pollard, R., and Borden, M. Ultrasound microbubble contrast agents: fundamentals and application to gene and drug delivery. *Annu Rev Biomed Eng* **9**, 415, 2007.
36. Froesch, E.R., Schmid, C., Schwander, J., and Zapf, J. Actions of insulin-like growth factors. *Annu Rev Physiol* **47**, 443, 1985.
37. Yoshinouchi, M., and Baserga, R. The role of the IGF-1 receptor in the stimulation of cells by short pulses of growth factors. *Cell Prolif* **26**, 139, 1993.
38. Cechowska-Pasko, M., Palka, J., and Bankowski, E. Glucose-depleted medium reduces the collagen content of human skin fibroblast cultures. *Mol Cell Biochem* **305**, 79, 2007.
39. Abramoff, M.D., Magelhaes, P.J., and Ram, S.J. Image processing with ImageJ. *Biophotonics Int* **11**, 36, 2004.
40. Thevenot, P., Nair, A., Dey, J., Yang, J., and Tang, L. Method to analyze three-dimensional cell distribution and infiltration in degradable scaffolds. *Tissue Eng Part C* **14**, 319, 2008.
41. Yang, J., Shi, G., Bei, J., Wang, S., Cao, Y., Shang, Q., Yang, G., and Wang, W. Fabrication and surface modification of macroporous poly(L-lactic acid) and poly(L-lactic-co-glycolic acid) (70/30) cell scaffolds for human skin fibroblast cell culture. *J Biomed Mater Res* **62**, 438, 2002.
42. Dey, J., Xu, H., Thevenot, P., Gondi, S., Nguyen, K., Summerlin, B., Tang, L., and Yang, J. Development of biodegradable crosslinked urethane-doped polyester elastomers. *Biomaterials* **29**, 4637, 2008.
43. Bryant, S.J., and Anseth, K.S. The effects of scaffold thickness on tissue engineered cartilage in photocrosslinked poly(ethylene oxide) hydrogels. *Biomaterials* **22**, 619, 2001.
44. Fournier, N., and Doillon, C.J. Biological molecule-impregnated polyester: an *in vivo* angiogenesis study. *Biomaterials* **17**, 1659, 1996.
45. Lo, H., Kadiyala, S., Guggino, S.E., and Leong, K.W. Poly(L-lactic acid) foams with cell seeding and controlled-release capacity. *J Biomed Mater Res* **30**, 475, 1996.
46. Whang, K., Tsai, D.C., Nam, E.K., Aitken, M., Sprague, S.M., Patel, P.K., and Healy, K.E. Ectopic bone formation via rhBMP-2 delivery from porous bioabsorbable polymer scaffolds. *J Biomed Mater Res* **42**, 491, 1998.
47. Tabata, Y., Nagano, A., and Ikada, Y. Biodegradation of hydrogel carrier incorporating fibroblast growth factor. *Tissue Eng* **5**, 127, 1999.
48. Jakobsen, J.A., Oyen, R., Thomsen, H.S., and Morcos, S.K. Safety of ultrasound contrast agents. *Eur Radiol* **15**, 941, 2005.
49. Porter, T.R., and Xie, F. Visually discernible myocardial echocardiographic contrast after intravenous injection of sonicated dextrose albumin microbubbles containing high molecular weight, less soluble gases. *J Am Coll Cardiol* **25**, 509, 1995.
50. Wei, G., and Ma, P.X. Structure and properties of nano-hydroxyapatite/polymer composite scaffolds for bone tissue engineering. *Biomaterials* **25**, 4749, 2004.
51. Goh, Y.Q., and Ooi, C.P. Fabrication and characterization of porous poly(L-lactide) scaffolds using solid-liquid phase separation. *J Mater Sci Mater Med* **19**, 1573, 2008.
52. Compton, S.J., and Jones, C.G. Mechanism of dye response and interference in the Bradford protein assay. *Anal Biochem* **151**, 369, 1985.
53. Woo, K.M., Chen, V.J., and Ma, P.X. Nano-fibrous scaffolding architecture selectively enhances protein adsorption contributing to cell attachment. *J Biomed Mater Res A* **67**, 531, 2003.
54. Kurita, R., Tabei, H., Iwasaki, Y., Hayashi, K., Sunagawa, K., and Niwa, O. Biocompatible glucose sensor prepared by modifying protein and vinylferrocene monomer composite membrane. *Biosens Bioelectron* **20**, 518, 2004.
55. Marois, Y., Chakfe, N., Guidoin, R., Duhamel, R.C., Roy, R., Marois, M., King, M.W., and Douville, Y. An albumin-coated polyester arterial graft: *in vivo* assessment of biocompatibility and healing characteristics. *Biomaterials* **17**, 3, 1996.
56. Tang, L., and Eaton, J.W. Fibrin(ogen) mediates acute inflammatory responses to biomaterials. *J Exp Med* **178**, 2147, 1993.
57. Hoeben, A., Landuyt, B., Highley, M.S., Wildiers, H., van Oosterom, A.T., and de Brujin, E.A. Vascular endothelial growth factor and angiogenesis. *Pharmacol Rev* **56**, 549, 2004.
58. Sakakibara, Y., Tambara, K., Sakaguchi, G., Lu, F., Yamamoto, M., Nishimura, K., Tabata, Y., and Komeda, M. Toward surgical angiogenesis using slow-released basic fibroblast growth factor. *Eur J Cardiothorac Surg* **24**, 105, 2003.
59. Maquet, V., and Jerome, R. Design of macroporous biodegradable scaffolds for cell transplantation. *Mater Sci Forum* **250**, 15, 1997.
60. Moore, K., MacSween, M., and Shoichet, M. Immobilized concentration gradients of neurotrophic factors guide neurite outgrowth of primary neurons in macroporous scaffolds. *Tissue Eng* **12**, 267, 2006.

Address reprint requests to:

Liping Tang, Ph.D.

Department of Bioengineering

University of Texas at Arlington

P.O. Box 19138

Arlington, TX 76019-0138

E-mail: ltang@uta.edu

Received: February 10, 2009

Accepted: March 27, 2009

Online Publication Date: May 11, 2009